MARINE GEORESOURCES & GEOTECHNOLOGY
https://doi.org/10.1080/1064119X.2017.1319448

Production key figures for planning the mining of manganese nodules

Sebastian Ernst Volkmann and Felix Lehnen

Institute of Mineral Resources Engineering (MRE), RWTH Aachen University, Aachen, Germany

ABSTRACT

Under the impression of decreasing ore grades and increasing production costs in conventional mining, seafloor minerals came into focus. Having gained a basic understanding of geological settings, there is still a lack of tools to assess and plan future mining projects in the deep-sea. This paper contributes to a mining concept which is inspired by the high-tech farming industry: strip mining. Potential mining fields are identified using image filters in conjunction with hydroacoustic backscatter data and slope angles and are portioned into long, narrow strips. In the framework of the EU-funded Blue Mining project, these methods were applied to a part of the eastern German exploration area, located in the manganese nodule belt of the Clarion Clipperton Zone, Pacific Ocean. Both, the mapping technique and the mining concept presented in this paper can be used in early-stage feasibility studies to derive estimates on production key figures for seafloor manganese nodule mining.

ARTICLE HISTORY
Received 17 December 2016
Accepted 11 April 2017

KEYWORDS
Deep-sea mining; manganese nodules; mine planning; production figures; resource mapping

Introduction

Even if 70% of our world's surface is covered by water, the deep-sea is in many ways the last great unexplored frontier on the Earth. However, the oceans hold a veritable treasure of valuable resources. Vast areas of ocean seafloor are covered by loose, metal-bearing nodules about the size of potatoes. Although seafloor manganese nodules (SMnN) were discovered by scientists of the HMS Challenger expedition (1872–76), it was Mero who advocated these deposits as a possible commercial source of metals in the early 1950s (Mero 1977). Since then, SMnN have been in the focus of numerous research projects, especially in the 1970s and 80s (Knodt et al. 2016). "The first attempt to exploit deep-sea manganese nodules ended in failure as a result of the collapse of world metal prices, the onerous provisions imposed by the *U.N. Convention on the Law of the Sea (UNCLOS)*, and the overoptimistic assumptions about the viability of nodule mining." (Glasby 2002) With the rising metal prices in 2006–2012, the interest in deep-sea mineral resources experienced a renaissance.

Seafloor manganese nodules contain primarily manganese, but also nickel, cobalt, copper, and rare earth elements (Hein 2013). Those deposits may be an important future source of supply for the Western European automotive, metal and electrical industries to sustain the expansion of renewable energies and climate (Wiedicke et al. 2015; Hein 2016; Marscheider-Weidemann et al. 2016). The International Seabed Authority (ISA) is the organ which is entitled to act on behalf of mankind and whose responsibility is to organize and control all mineral-related activities and resources in "the Area" beyond the limits of national jurisdiction (United Nations 1982). In that time the EU funded several projects related to deep-sea mining as a part of their research and technological development program. The most recent projects are MIDAS (2013–2016), Blue Mining (2014–2018), and Blue Nodules (2016–2020).

While today's mine planning of land-based ore deposits follows methods which are well established (Darling 2011), mining standards for the deep-sea have yet not been established. The identification of (potentially) mineable seafloor area is reliant on a project's exploration data. Kuhn, Rühlemann, and Wiedicke-Hombach (2012) "[…] suggest that hydroacoustic backscatter data in conjunction with slopes less than 3° are indicative of prospective Mn nodule fields." This approach is further developed and refined to identify potentially mineable areas and to define mining fields. Inspired by the high-tech farming industry, additional information is derived regarding mineable proportions, field sizes, and field characteristics. Suitable mining patterns can then be assessed using production key figures (PKFs). Thus, this paper contributes to the setting of requirements and the validation of assumptions for future mine planning in the deep-sea.

Background

This paper uses background data of the Blue Mining project, which received funding from the European Commission (EC) as a part of the 7th Framework Programme for Research and Technological Development. The Blue Mining deposit model for SMnN was prepared by Rahn (2016). Further characteristics of the deposit were provided by the Federal Institute for Geosciences and Natural Resources (BGR).

CONTACT Sebastian Ernst Volkmann volkmann@mre.rwth-aachen.de Institute of Mineral Resources Engineering (MRE), RWTH Aachen University, Institute of Mineral Resources Engineering (MRE), Wüllnerstr. 2, 52062 Aachen, Germany.
Color versions of one or more of the figures in the article can be found online at www.tandfonline.com/umgt.

Blue mining concept

Started in February 2014, the EU-funded Blue Mining project (breakthrough solutions for the sustainable exploration and extraction of deep-sea mineral resources) addresses all aspects of the value chain in this field, from resource discovery to production assessment and from exploitation technologies to the legal and regulatory framework. An international European consortium of 19 enterprises and research organizations out of various maritime fields of expertise is jointly investigating sustainable approaches. In the technical part, Blue Mining is focusing the development of a vertical transport system (VTS). Two different technologies are considered: An airlift and a serial centrifugal pump system. In case of the airlift system, compressed air is injected at one (or more) points of the vertical riser to reduce the density of the slurry, containing SMnN. Instead of booster stations, as being used for the hydraulic pump system, compressors are installed on deck of the mining support vessel (MSV) to generate compressed air. The VTS is designed for production rates of up to 150 kg/s (dry solids). This should enable annual production rates of up to two million dry metric tons of ore.

The Blue Mining concept (Figure 1) is based on routines used in the high-tech farming industry. The concept was jointly developed by following entities: RWTH Aachen University, Royal IHC, MTI, Dredging International (DEME), Ramboll IMS, and MH Wirth. The proposed mining system composes of one or two self-propelled, crawler-type seafloor mining tools (SMTs) and different types of underwater vehicles. Autonomously or remotely operated vehicles (AUVs/ROVs) will be required to execute specific tasks such as salvage of equipment, repair, and maintenance as well as for exploration and environmental monitoring. Mining is planned in designated areas. A strip-like mining pattern is considered, whereby the MSV follows the mining route of the SMT. SMnN are picked up by the SMT, freed from sediments, and sized. The ore is then hydraulically lifted on board of the MSV as a mixture of seawater and broken SMnN, diluted by a smaller amount of fine sediment. On board of the MSV, the slurry is dewatered, bunkered, and discharged onto bulk carriers for shipment to the purchaser. Seawater and residual particles from the dewatering process are pumped back close to the ocean floor to reduce the spread of particle-laden plumes and thus environmental impact. Processing and refining of ore is not subject to Blue Mining research.

Deposit characteristics

The German license area in the eastern part of the Clarion Clipperton Zone (CCZ; 11°00′N, 118°00′W; Figure 1) encompasses a total of 75,000 km^2. The license area is divided into two regions with 17,000 km^2 in the central part and 58,000 km^2 in the eastern part of the Pacific Nodule Belt (Rühlemann et al. 2011). For spatial analysis, exploration data of the eastern German exploration license (E1) have been used. A vessel-based bathymetric survey was executed by the BGR using the swath echo sounding system EM 120 to receive information on the geological properties of the seafloor (Kuhn, Rühlemann, and Wiedicke-Hombach 2012). "The seafloor is characterized by extensive deep-sea plains interspersed with elongated NNE-SSW oriented horst and graben structures that are several kilometers wide, tens of kilometers long and on the order of hundred meters high […] An analysis of the topography shows that in ~80% of the license area the slope of the seafloor does not exceed 3°." (Rühlemann et al. 2009)

In the framework of the Blue Mining project, a potential mine site within E1 was studied (Rahn 2016). Due to its size (255 km^2) the exemplary mine site is assumed to represent the characteristics of a potential mining field (Table 1). "The

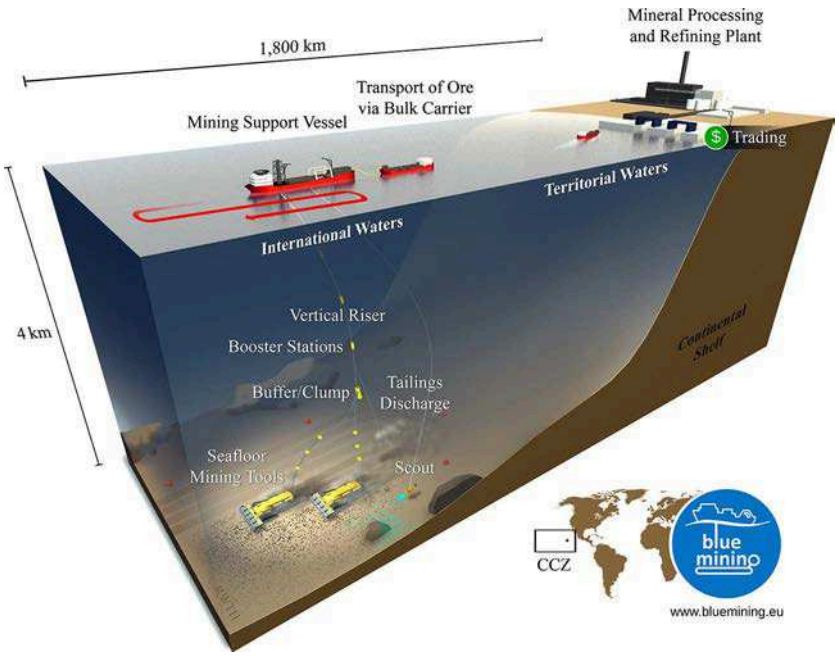

Figure 1. Strip mining concept for SMnN proposed by Blue Mining. *Note*: SMnN, seafloor manganese nodules.

Table 1. Characteristics of E1 (BGR) and of the exemplary mine site of the Blue Mining project (Rahn 2016).

Item	Values		Unit
	German exploration area E1	Exemplary mine site within E1	
Area	58,000	255	km^2
Depth	1,460–4,680 (4,240)	3,987–4,022	m
Nodule abundance[a]	0–23.6 (13.7)	10.3–21.3 (16.5)	kg/m^2, dry
Copper, nickel and cobalt grades[a]	1.22–3.45 (2.75)	2.58–3.13 (2.84)	%
Manganese grade[a]	20.5–40.3 (31.3)	— (29.3)	%
Total tonnage of nodules	560	4	Mt, dry
Copper, nickel, and cobalt tonnage	14	0.11	Mt
Manganese tonnage	159	1.17	Mt

[a]Arithmetic mean (average value) in brackets.

study area is dominantly flat, 94% of the area exhibit a slope of less than 3°, only 6% of the area has a slope larger than 3° with a maximum of 29.86°. The nodule coverage is on average 16.51 kg/m^2 with a minimum of 10.29 kg/m^2 and maximum of 21.31 kg/m^2 (dry weight). The total tonnage of nodules is about 4 Mt with 113,812 t for copper, nickel, and cobalt tonnage and 1,171,000 t for manganese." (Rahn 2016)

Ordinary kriging interpolation was applied to predict nodule abundances on the basis of box core sample data provided by the BGR (Rahn 2016). The created prediction map (Figure 2) indicates large continuous areas of nodule abundances between 14–16 and 16–18 kg/m^2. The chemical composition of the SMnN is relatively constant. The coefficient of variation for nodule abundance is about seven times higher (0.25) than compared to the coefficient of variation for the combined grade (Co + Cu + Ni) (Rahn 2016). At this planning stage, it is considered to bulk-mine a field irrespective of metal grades.

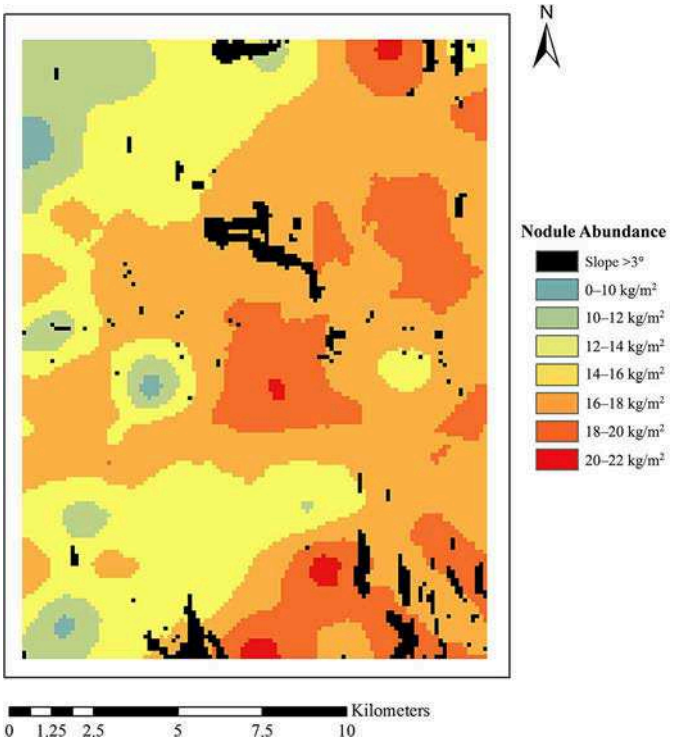

Figure 2. Prediction map on nodule abundance after Rahn (2016).

Methodology

This section provides definitions and develops formulas for the proposed mining concept and PKFs as well as definitions pertaining to spatial (image) analysis. Definitions on the mining capacity, rate, and field efficiency were adopted from agriculture and high-tech farming industry (Grisso, Jasa, and Rolofson 2000; Hunt and Wilson 2015; Hanna 2016). The approach was then tested for a part of the eastern German license area (E1), in which context PKFs were estimated.

Definitions

Out of the previously described mining concept, certain definitions can be derived. Accordingly, a definition of resources and reserves is formulated. Both groups of definitions are then processed within the calculation of PKFs.

Mining concept

"Strip mining" is a proposed mining method for deep-sea mining which involves mining a field partitioned into long, narrow strips, similar to practices in farming as described by Hunt and Wilson (2015). A strip-like mining pattern is suggested for harvesting SMnN.

The "mine plan" is considered as a map, which shows all relevant information to execute a mining project. Details of the seafloor, e.g., on nodule abundance and grades are stored as raster data. Accordingly, the seafloor is divided into several raster units. Besides geological information, mine sites, mining fields, and mining routes are outlined (Figure 3).

A "mine site" is defined as an area on the ocean floor where, under specific geological, technical, and economic conditions, a single SMnN mining operation (one MSV) can be performed for a period of time (UNOET 1987).

A "mining field" is defined as the next smaller unit in a mine site. It refers to a continuous mineable area described by a boundary, which defines the "in-field" reserve. Thus, a mine site may contain several mining fields.

A "strip" is defined as the next smaller unit within in a mining field. It is characterized by width and a path with a starting point and an end point, representing turning or field

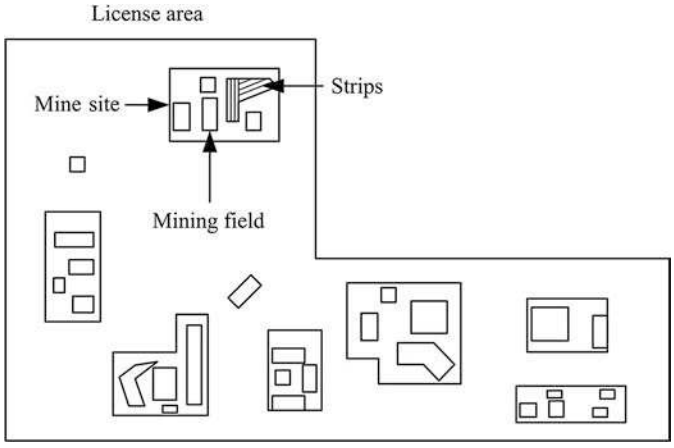

Figure 3. Schematic illustration of a mine design for SMnN. *Note*: SMnN, seafloor manganese nodules.

entry and exit points of the SMT. SMTs are navigated along predefined mining routes, which reflect the mining pattern (Figure 1).

A "raster unit" is defined as a quadratic cell of a grid into which the seafloor is divided. It contains information on the area, e.g., obtained from vessel-based bathymetric and near-seafloor AUV-based surveys. In this study, grid spacing is restricted by the spatial resolution. Raster units are hereinafter represented by image pixels.

Resources and reserves

To dimension a corresponding mining system which would best utilize the mineral deposit, SMnN in the potentially mineable area are qualified as potential reserves. However, none of the known SMnN resources have reached the status of a reserve, yet. This is due to the lack of economic technological readiness and a missing legal framework for the exploitation of SMnN (mining code). If not stated otherwise, nodule abundance and metal grades refer to the dry weight. Occasionally, nodule abundance is expressed in wet weight per unit surface area. The reduction factor used to arrive at the former is approximately 0.7 (UNOET 1987). Average values refer to the arithmetic mean.

The "resource" (RSC) is defined as the quantity of SMnN contained in a particular area (A_{TOT}) with prospect for eventual economic extraction. In general, mineral resources are subdivided into inferred, indicated, and measured resources in order of increasing geological confidence (Rendu and Miskelly 2013). The quantity of SMnN in the area is estimated on the basis of the average nodule abundance and size of the area (Formula 1).

Formula 1: Quantity of SMnN in the mine site or license area.

$$RSC = NA_{TOT} \times A_{TOT} \times 10^3$$

where RSC = resource (t, dry weight), NA_{TOT} = average nodule abundance in the total area (kg/m^2, dry weight), A_{TOT} = total area (km^2), and 10^3 = conversion from kg to t and from km^2 to m^2.

The "reserve" (RSV) is defined as the quantity of SMnN contained in the mineable proportion of a particular area (A_{TOT}). In general, a reserve represents the probable or proven mineable share of a mineral resource "[…] taking into account all relevant metallurgical, economic, marketing, legal, environmental, social and governmental factors." (Rendu and Miskelly 2013) Beside general criteria, area-specific criteria apply, distinguishing between mineable and nonmineable seafloor (Formula 5). The quantity of SMnN in the potentially mineable area is again estimated on the basis of the average nodule abundance and size of the area (Formula 2).

Formula 2: Quantity of SMnN in the mineable area.

$$RSV = NA_M \times A_M \times 10^3$$

where RSV = reserve (t, dry weight), NA_M = average nodule abundance in the mineable area (kg/m^2, dry weight), A_M = mineable area (km^2).

The "in-field reserve" (RSV_F) is defined as the quantity of SMnN contained in the mining fields (A_F). Mining fields are those fields of the mineable area that are actually mined. Expecting a field to be bulk-mined, it is assumed that the average nodule abundance in the field is equal to the abundance in the covered area. The quantity of SMnN in the fields is estimated on the basis of average nodule abundance and the total size of the fields (Formula 3).

Formula 3: Quantity of SMnN in the mining fields.

$$RSV_F = NA_F \times A_F \times 10^3$$

where RSV_F = in-field reserve (t, dry weight), NA_F = average nodule abundance in mining fields (kg/m^2, dry weight), A_F = area of mining fields (km^2).

The "gross mineable proportion" (α) is defined as the percentage of the seafloor (A_{TOT}) which meets all criteria of being mineable (Formula 4). In image or spatial analysis, the gross mineable proportion is estimated by dividing the number of mineable raster units (cells or image pixels) by the total number of units in the particular area.

Formula 4: Gross mineable proportion.

$$\alpha = \frac{A_M}{A_{TOT}} \times 100\%$$

where α = gross mineable proportion (%).

The "mineable area" (A_M) corresponds to the former definition but is expressed in square kilometers. A raster unit (cell or pixel) may not be mineable due to its economic value, environmental protection, or inaccessibility (water depth, slope, or obstacles in that area like cliffs, pot holes, and scarps). The approach (Formula 5) can be found in another form at UNOET (1987). In this study, exclusion criteria (crit i) are based on backscatter data, slope angles, and calculated density values. To avoid multiple counting, the set union is used here instead of the sum of areas fulfilling criteria:

Formula 5: Mineable area.

$$A_M = A_{TOT} - \bigcup_{i=1}^{n} A_{Crit\ i}$$

where n = number of exclusion criteria, $A_{Crit\ i}$ = area excluded from mining by criterion i (km^2).

The "net mineable proportion" (β) is defined as the percentage of seafloor (A_{TOT}) where mining would actually be performed (A_F; Formula 6). In image or spatial analysis, the net mineable proportion is estimated by dividing the number of raster units (cells or image pixels) planned to be mined by the total number in the area.

Formula 6: Net mineable proportion.

$$\beta = \frac{A_F}{A_{TOT}} \times 100\%$$

where β = net mineable proportion (%).

Development of production key figures

"Production key figures are used to describe production processes (that is, how much of each component or raw material is consumed during which period, at which location, and in which production process) as well as how much output

quantity is produced." (SAP 2014) PKFs considered for planning the mining of SMnN are the production rate, yield per area, duration of mining, seafloor consumption and requirement. Time and seafloor are consumed during mining, whereas yield and production describe output quantities. Moreover, resource utilization, mining efficiency and extraction efficiency are calculated. The latter describe how efficiently the operation performs and how efficient the mineral deposit is utilized. Thus, these figures refer to key performance indicators.

The "production rate" (P) is defined as the dry mass of SMnN recovered per unit of time. It is expressed in kilograms of dry solids per operational second. The production rate is controlled by the mining rate, nodule abundance, and collecting efficiency in the area covered (Formula 7). Dilution of ore with sediments and transport losses are neglected. The production rate is constrained by the mining capacity (MR_{Max}) and the production capacity (P_{Max}).

Formula 7: Production rate.

$$P = NA \times MR \times \eta_C$$

where P =production rate (*kg/s, dry weight*), NA = nodule abundance (*kg/m², dry weight*), MR = mining rate (*m²/s*), see Formula 9, and η_C = collecting efficiency (%).

The "production capacity" (P_{Max}) is defined as the maximum dry mass of SMnN recovered per unit of time. It is expressed in kilograms of dry solids per operational second. It is technically constrained by the lifting capacity (VTS_{Max}) or the collecting capacity (SMT_{Max}). Hereinafter, it is assumed that production is limited by the lifting capacity of the VTS.

The "annual production rate" (P_A) is defined as the dry mass of SMnN, in (million) dry metric tons, recovered per calendar year. It is estimated on the basis of average nodule abundance in the mining fields, annual operating time, average mining rate, and collecting efficiency (Formula 8). The formula can also be used to determine the required average nodule abundance to meet the production target.

Formula 8: Annual production rate.

$$P_A = NA_F \times T \times MR_A \times \eta_C \times 3.6$$

where P_A = annual production rate (t/a, dry weight), T = annual operating time (scheduled) (h/a), MR_A = annual average mining rate (m^2/s), see Formula 10, and 3.6 = conversion from kg to t and from s to a.

The "mining rate" (MR) is defined as the effective rate of coverage in square meters per second. It is the product of the effective collecting width and collecting speed during operation (Formula 9).

Formula 9: Mining rate.

$$MR = w \times v$$

where w = collecting width (m) and v = collecting speed (m/s).

The "mining capacity" (MR_{Max}) is defined as the maximum mining rate in square meters per second. It is obtained when operating at full capacity utilization, i.e., full operating width and full rated collecting speed.

The "average mining rate" (MR_A) is defined as the average area mined during the time the machine is committed to the operation. It is estimated on the basis of mining capacity and annual time efficiency (Formula 10).

Formula 10: Annual average mining rate.

$$MR_A = MR_{Max} \times \eta_T$$

where MR_{Max} = mining capacity of the SMT(s) (m^2/s) and η_T = time efficiency (%).

The "time efficiency" "[…] is a percentage reporting the ratio of the time a machine is effectively operating to the total time the machine is committed to the operation." (Hunt and Wilson 2015) Hereinafter, it is referring to the ratio of the annual operating time at full mining capacity to the scheduled operating time (Formula 11). Field-to-field travel is counted as productive time, when collecting ore.

Formula 11: Time efficiency.

$$\eta_T = \frac{T_{MC}}{T} \times 100\%$$

where T_{MC} = annual operating time at mining capacity (i.e., maximum mining rate) (h/a).

The "resource utilization" (RU) is defined as the percentage of SMnN recovered from an area (Formula 12).

Formula 12: Resource utilization.

$$RU = \frac{RSV}{RSC} \times e = \frac{Y}{RSC} \times 100\%$$

where RU = resource utilization (%), Y = yield of SMnN (t, dry weight), see Formula 13, and e = extraction efficiency (%), see Formula 15.

The "theoretical resource utilization" (RU_{Max}) is defined and calculated accordingly, assuming an ideal extraction efficiency ($e = 100\%$). It is used in assessing the potential of a given resource against an envisaged production and mining rate.

The "yield" (Y) is defined as the quantity of SMnN recovered from an area, expressed in dry metric tons. In agriculture, yield is a measure which refers to the yield of crop per unit of land (Hunt and Wilson 2015). It is here estimated on the basis of average nodule abundance, size of area, net mineable proportion, and in-field mining efficiency (Formula 13). Alternatively, latter could be replaced by the gross mineable proportion and overall mining efficiency.

Formula 13: Yield per area.

$$Y = NA_F \times A_{TOT} \times \beta \times \eta_{MF} \times 10^3$$

where η_{MF} = in-field mining efficiency (%), see Formula 16.

The "duration of mining" (D) in one operation is estimated on the basis of estimated yield and envisaged annual production rate (Formula 14).

Formula 14: Duration of a single mining operation.

$$D = \frac{Y}{P_A}$$

where D = duration of mining operation (a).

The "extraction efficiency" (e) is defined as the percentage of SMnN recovered from the mineable area. It is thus the relation of yield and reserve. Alternatively, it can be calculated

on the basis of overall mining efficiency, average nodule abundance in the mineable area, and in the mining fields (Formula 15).

Formula 15: Extraction efficiency.

$$e = \frac{Y}{RSV} \times 100\% \ = \frac{NA_F}{NA_M} \times \eta_M$$

where: η_M = overall mining efficiency (%), see Formula 17.

The "in-field mining efficiency" (η_{MF}) is defined as the mining efficiency, in percent, achieved in the mining fields (A_F). It is the product of the area coverage performance and collecting efficiency (Formula 16). It indicates the technical and operational efficiency of the extraction process in the mining fields. As a field is intended to be bulk-mined, it is equal to the extraction efficiency in a field.

Formula 16: In-field mining efficiency.

$$\eta_{MF} \ = \eta_C \times \eta_A$$

where: η_A = area coverage performance (%).

The "overall mining efficiency" (η_M) is defined as the product of the technical collecting efficiency, the operational area coverage performance, and the spatial utilization of mineable area (Formula 17). Unlike the extraction efficiency (e), it indicates the overall efficiency of the mining process in the mineable area, but independent of where mining is performed and regardless of nodule abundance.

Formula 17: Overall mining efficiency.

$$\eta_M \ = \eta_C \times \eta_A \times \varphi$$

where φ = utilization of mineable area (%), see Formula 18.

The "collecting efficiency" (η_C) or "pickup efficiency" is defined as the percentage of SMnN recovered from the seafloor. It is primarily a technical parameter, which depends on, inter alia, the collecting technique, collecting speed, size, and burial depth of the SMnN (Hong et al. 1999; Yamazaki 2008). The collecting efficiency is assumed to be constant for the scope of this study.

The "area coverage performance" (η_A) is defined as the percentage of a designed field actually covered by the SMT. It reflects the accuracy of the operator and the SMT(s) in covering all margins of the planned field while harvesting.

The "utilization of mineable area" (φ) is defined as the share of actual mining fields in a generally mineable area. Thus, it indicates the percentage of a mineable area being utilized, taking into account the engineered field design of the mine plan. Accordingly, φ can be calculated as the ratio of the net mineable to the gross mineable proportion (Formula 18).

Formula 18: Utilization of mineable area.

$$\varphi \ = \frac{\beta}{\alpha} \times 100\%$$

The "annual consumption of seafloor" (A_M^*) is defined as the required area to yield in a certain annual production rate. It is estimated on the basis of annual production rate (target value), average nodule abundance in the mining fields, and collecting efficiency (Formula 19).

Formula 19: Annual consumption of seafloor.

$$A_M^* = \frac{P_A}{NA_F \times \eta_C \times 10^3}$$

where A_M^* = annual consumption of seafloor (km^2/a).

The "total seafloor requirement" (A_{TOT}^*) is defined as the total area required performing a single mining operation. It is estimated on the basis of annual production (target) rate, envisaged life of mine, average nodule abundance in the mining fields, net mineable proportion, and in-field mining efficiency (Formula 20). Alternatively, latter could be replaced by the gross mineable proportion and overall mining efficiency. The formula has already been published in different forms (UNOET 1987).

Formula 20: Total seafloor requirement.

$$A_{TOT}^* = \frac{P_A \times D}{NA_F \times \beta \times \eta_{MF} \times 10^3}$$

where A_{TOT}^* = total seafloor requirement (km^2).

Computational image analysis

GIS software applications already provide a wide spectrum of tools to perform spatial analysis but do not always allow for modification or require expertise. In this paper, spatial analysis is performed through image analysis of GIS-data. The authors present their own programmed tools, i.e., filters involving spatial analysis of an (image) area. The identification of mineable areas and fields follow these steps.

Creating a binary image

The presented mapping approach was adopted from methods proposed by Rühlemann et al. (2013) and Kuhn, Rühlemann, and Wiedicke-Hombach (2012). "High-resolution side-scan sonar data, seafloor photographs as well as box core sampling proved that manganese nodule fields with an abundance of $>$ 10 kg/m^2 can be distinguished from sediment-covered seafloor areas devoid of nodules using backscatter data." (Kuhn, Rühlemann, and Wiedicke-Hombach 2012) The "seafloor backscatter" "[…] is defined as the amount of acoustic energy being received by the sonar after a complex interaction with the seafloor. This information can be used to determine bottom type, because different bottom types 'scatter' sound energy differently." (Stuart 2011)

Kuhn, Rühlemann, and Wiedicke-Hombach (2012) created a binary image on the basis of hydroacoustic backscatter data and slope angles for a part of E1. A "binary image" is a digital black-and-white image. This requires that raster data are translated into binary information. Hereinafter, a valid (white) image pixel represents a mineable raster unit, whereas a non-mineable raster unit is represented by an invalid (black) image pixel. A valid pixel (white; mineable) refers to a backscatter value between 70 and 140 ($>$10 kg/m^2, wet weight) and a slope $\leq$3°. An invalid pixel (black; nonmineable) is outside this range or/and $>$3° (Kuhn, Rühlemann, and Wiedicke-Hombach 2012). The slope angle (in degrees) is derived from raster bathymetry data.

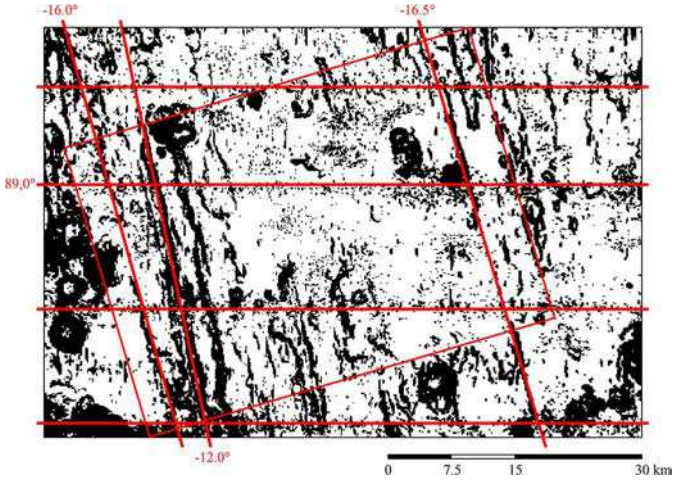

Figure 4. Binary image of the bathymetry of the seafloor in a part of E1 analyzed by Kuhn, Rühlemann, and Wiedicke-Hombach (2012). The inner rectangle indicates the analyzed area. Lines represent interpreted horizontal and vertical image structures.

Within the scope of this study, a part of this area was analyzed (Figure 4). The cropped image consists of 416 × 298 pixels, equivalent to approximately 1,800 km^2. The spatial resolution is given with 120 m × 120 m per pixel. The ore layer is assumed to be uniformly graded.

Image filtering

The Blue Mining concept requires that continuous areas are identified, which would allow mining for a period of time. For this purpose, the so-called "neighborhood" filters were applied to the binary image. In image processing, filtering is a technique for modifying or enhancing an image. Within the scope of this study, custom-made filters were programmed to determine the concentration of valid pixels: a "neighborhood filter" is a moving, overlapping statistical analysis method. A density value is calculated for each valid image pixel, which falls into the search area. Values are translated into grayscale color values. The "search area" is thus the neighborhood of an image pixel and is described by the search distance. The "search distance" is again the distance (DIST) originating from the center pixel to the border pixel (Figure 5). The center pixel is not considered in the distance value.

The circular (CIR-) filter is the simplest filter, which uses a circular search area. In addition to the latter, a bidirectional (VER-) filter was developed to simulate a strip-like mining pattern, portioning the area into narrow strips. Using this filter, the search distance which originates in backward and forward directions from the center pixel and the rotation angle theta (ϑ) must be parameterized. The "angle theta" is the angle from the y-axis winding clockwise in screen space. It is oriented to the main structures interpreted from the original binary image (Figure 4) and is −16.5°.

Strictly speaking, the filter works only in vertical direction (DIST-V) as the background image is rotated relative to the search direction. To consider mine planning, it is assumed that nonmineable areas, i.e., pixels must be bypassed by the SMT (s). To take this into account, a search in horizontal direction (DIST-H) was implemented. Furthermore, the circular (CIR-) filter and the bidirectional (VER-) filter were combined. This is hereinafter referred to a combined (MIX-) filter.

A grayscale image is created from the binary image. A pixel remains mineable if a certain percentage of neighboring pixels are mineable. The mineable area is subdivided into two types of areas by defining two threshold values (TRH1, TRH2). Light gray (LGY) pixels represent density values ≥ TRH1 and <TRH2, whereas white (WT) pixels refer to values > TRH1 and ≤100%. It is assumed that mining operation would be performed in core areas with a high density of valid pixels (WT), whereas secondary areas (LGY) are considered for maneuvering or/and may serve as a buffer zones. Black pixels (BK) are assumed to be not mineable. A TRH1-value of 80% and a TRH2-value of 90% are considered to best reflect the requirements and risks of a pioneer deep-sea mining operation.

Field design

Field design is only merely hinted because the planning of a field is not within the scope of this study. The color transitions in the processed images outline the contours of potentially mineable fields, before field design. It was assumed that a mining field would be portioned into narrow, most longish strips to reduce the number of turnings. To take this into account, field boundaries are described by a simple geometry.

Results

Production key figures are now exemplarily calculated on assumptions made by the Blue Mining concept and the area (E1) studied (Table 2). The same applies for the image analysis which has been applied to actual data out of E1.

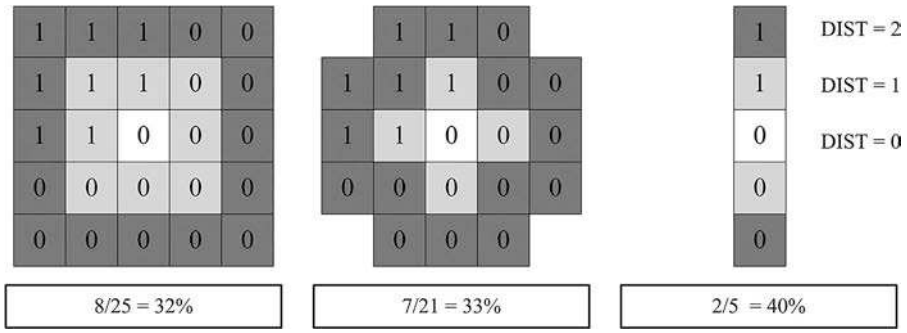

Figure 5. Schematic illustration on the calculation of the density value for a rectangular, circular, and vertical filter shape.

Table 2. Key assumptions for the calculation of production key figures.

Item	Value	Unit
Annual production rate (P_A)	1.5–2	Mt/a, dry
Operating time (T)	5,000	h/a
Mining capacity (MR_{Max})	9	m^2/s
Collecting efficiency (η_C)	80	%
Area coverage performance (η_A)	75–95	%
Lifting capacity (VTS_{Max})	150	kg/s, dry
Average abundance in the mineable area (NA_M)	13.7	kg/m^2, dry
Average abundance in the mining fields (NA_F)	13.7–16.5	kg/m^2, dry

Spatial analysis

Processed images were analyzed for different filter settings, computing the gross and net mineable proportion by counting the total, the valid and nonvalid numbers of pixels contained in the image. Early results indicated that a value of −16.5° for ϑ was already an appropriate approximation to obtain the maximum mineable proportion and was therefore retained. Secondary area is only indicated in processed images. In all other cases, TRH2 is equal to TRH1. Processed images are presented to allow a visual comparison of different filter settings. A red rectangle indicates the area where confident density values can be expected. For pixels outside the rectangle, not all neighboring pixels are defined as out of the image and were excluded from calculation. Uncertainty was not quantified.

Results of the image analysis show that 70% (α) of the analyzed area is potentially mineable (Figure 6). In general, one can state: the higher the threshold level, the lower the mineable proportion and vice versa. The circular filter (Figure 6a) is not efficient compared to the other filters. This is in particular evident for larger vertical search distances (V-DIST). Highest values are obtained by application of the bidirectional filter (-Figure 6b) and the combined (MIX-) filter (Figure 6d).

Processed images (Figure 7) indicate potentially mineable areas, filtered by using a circular (CIR-) filter, bidirectional (VER-) filter, and combined (MIX-) filter. The mineable proportion ranges between values of 30 and 45%. Narrow areas, which are potentially mineable, are not detected using the circular (CIR-) filter (Figure 7a). The less fringed the mineable area, the higher the horizontal search distance (Figure 7b and 7c). The image created by applying the combined filter (Figure 7d) is like the first one but shows narrow details. As determined for the combined (MIX-) filter, the core area increases by the factor 2, whereas the secondary area remains almost the same.

Within the analyzed area, 28 potential mining fields were identified, covering 36% (β) of the total area (Figure 8). The typical size of a potential mining field would be about 25 km^2. These fields would be 1–4 km wide and 5–14 km long (average value ± the standard deviation), north–south orientated. The biggest field would cover an area of 114 km^2 and would sustain mining for almost 1 year, assuming 250 days of operation per calendar year.

Production key figures

Production

Blue Mining aims for an annual production of 1.5 up to 2 Mt SMnN (P_A). PKFs can be derived accordingly. Mining is scheduled 250 days and 20 hours per day. Planning with 5,000 operating hours per year (T), 400 dry metric tons of SMnN must be collected on average per operating hour (P) to realize 2 Mt/a. The lifting capacity (VTS_{Max}) considered by Blue Mining is 150 kg/s. Full capacity utilization would be achieved by operating at 10 m^2/s and 19 kg/m^2, 8 m^2/s and 24 kg/m^2 or 6 m^2/s and 24 kg/m^2 (Figure 9). Average mining rates (MR_A) of at least 6–10 m^2/s must be achieved when mining average nodule abundances of 13.7–16.5 kg/m^2 to realize 1.5–2 Mt/a (Figure 10).

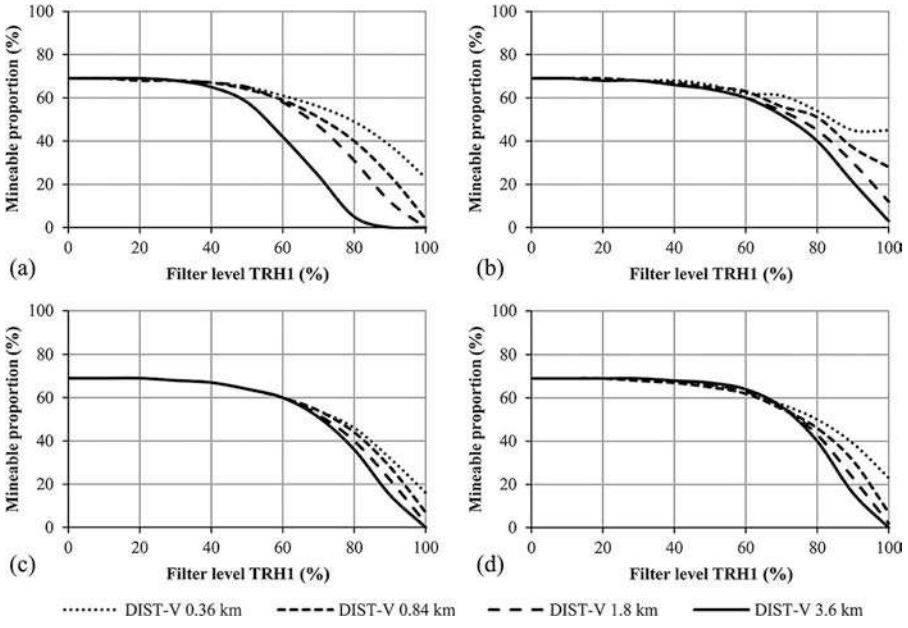

Figure 6. Potentially mineable proportion computed for the study area. (a) Radial filter. (b) Bidirectional filter. (c) Bidirectional filter with a horizontal distance of 0.36 km. (d) Mixture of a radial and bidirectional filter (for all: $\vartheta = -16.5°$, TRH2 = TRH1, DIST-V is the vertical filter distance).

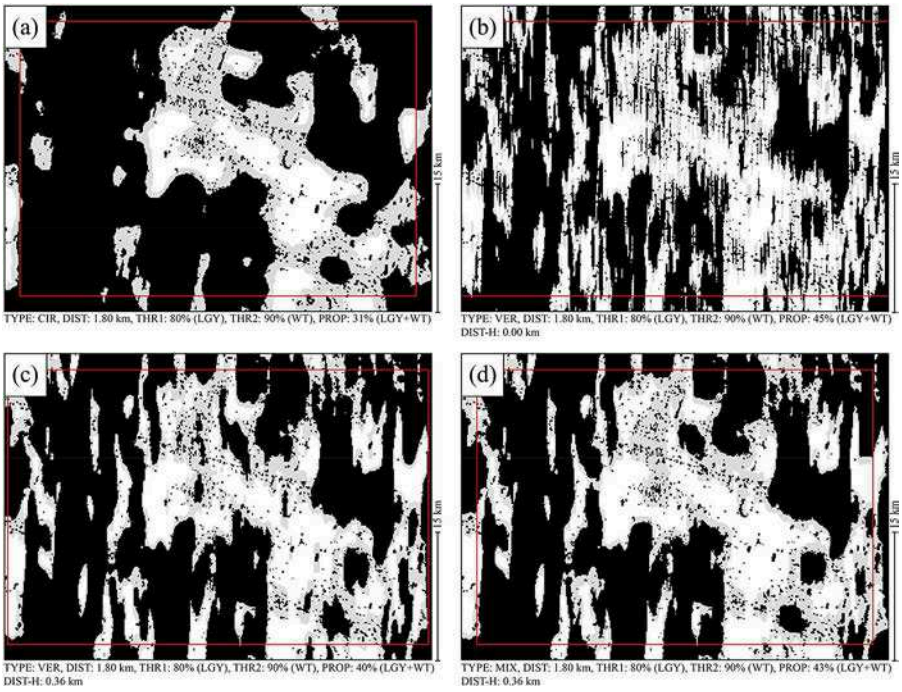

Figure 7. Potentially mineable area computed for the study area. (a) Radial filter. (b) Bidirectional filter. (c) Bidirectional filter with a horizontal distance of 0.36 km. (d) Mixture of a radial and bidirectional filter (for all: $\vartheta = -16.5°$, TRH2 = TRH1). Black (BK): nonmineable area. Light gray (LGY): 80–89% of the surrounding area is mineable; white (WT) if higher. The inner rectangle indicates the effective filter area.

Resource utilization

The theoretical resource utilization (RU_{Max}) is dependent on the set cutoff nodule abundance, here shown exemplary for the area studied by Rahn (2016). A decrease in resource utilization from about 90 to 20% can be seen when increasing the cutoff value from 14 to 18 kg/m^2 (Figure 11). The higher the cutoff nodule abundance, the more areas are not mined. Considering the assumptions made (upper abundance of 16.5 kg/m^2), a cutoff of about 10.3 kg/m^2 would apply, leading to a theoretical RU of 100%. To meet the production requirements, mining must focus on areas of adequate average nodule abundance. For scenarios of different average abundances, RU_{Max} can be derived accordingly (Table 3). Figures of nodule abundances are labeled with the symbols A*, A, B, and C which reflect the likeliness of occurrence, based on literature and Blue Mining results (Rahn 2016).

Mining and extraction efficiency

The gross mineable proportion (α) is computed to be 70%, whereas the net mineable proportion (β) is 36% in case all mining fields are mined. It is shown how mining efficiency would change if strips would intentionally were left unmined (Table 4). Such zones may provide connectivity of habitat for native species or unintentionally left unmined due to imprecise navigation of the SMT(s). In the base case, the coverage performance (η_A) is assumed to be 95%. Leaving a 5-m-wide strip unmined next to each strip mined, this would reduce area coverage by approximately 20%. The strip width is assumed to be 20 m. This corresponds to the collecting width of the SMT(s) considered by Blue Mining. A collecting efficiency (η_C) of 80% is assumed.

The mining efficiency (η_{MF}) is estimated to be about 60–76% in the fields and approximately 30–40% in total (η_M).

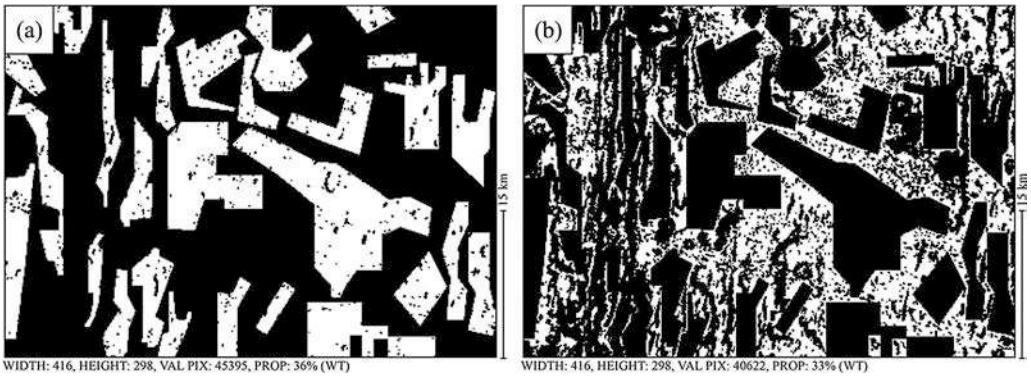

Figure 8. Area before (a) and after mining (b) computed for the study area. (a) Mineable area inside the fields in white (WT). Nonmineable area inside and areas outside the fields in black (BK). (b) Extraction losses in white (WT). Nonmineable area and fields mined in black (BK).

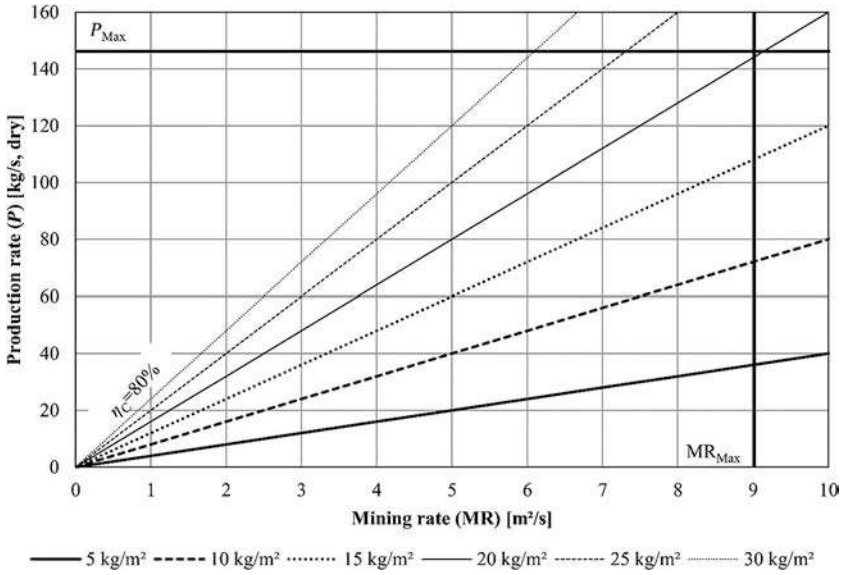

Figure 9. Production (P) as a function of nodule abundance (NA) and mining rate (MR) at a constant collecting efficiency (η_C) of 80%. Production is limited by the production capacity (P_{Max}) and mining capacity (MR_{Max}) exemplary for the Blue Mining project.

Based on the assumption that the average nodule abundance in the mineable area (NA_M) would be 13.7 and 16.5 kg/m^2 in the fields (NA_F) at the best, the extraction efficiency (e) is estimated to be slightly higher: approx. 30–50%.

Yield and duration of mining

The total area of the analyzed part of E1 (A_{TOT}) amounts to almost 1,800 km^2. Assuming the average nodule abundance in the fields (NA_F) to range between 13.7 and 16.5 kg/m^2, about 5–8 Mt of SMnN could be recovered (Y). Thus, the area may provide enough SMnN to sustain mining for approximately 2½–5½ years (D), entailing production rates (P_A) of 1.5–2 Mt per year and overall mining efficiencies (n_M) between about 30 to 40%.

Seafloor consumption and requirement

Seafloor consumption (A^*_M) depends on the average abundance in the mining fields harvested by the miner. A higher average abundance leads to lower consumption and vice versa (Table 5). To achieve a production of 1.5–2 Mt per year, it is estimated that approximately 114–182 km^2 would have to be mined per year. Planning with 250 days per year, about 64–102 soccer fields (68 × 105 m^2) would have to be mined per day. The area mined in a period of 20 years is estimated to be about 2,300–3,600 km^2. This is about the size of Luxembourg and represents only about 4–6% of E1. The total seafloor requirement (A^*_{TOT}) is estimated to make up between 12 and 24% of E1. Absolute values may range between 6,500 and 14,100 km^2, entailing 20 years of production at annual rates between 1.5 and 2 Mt.

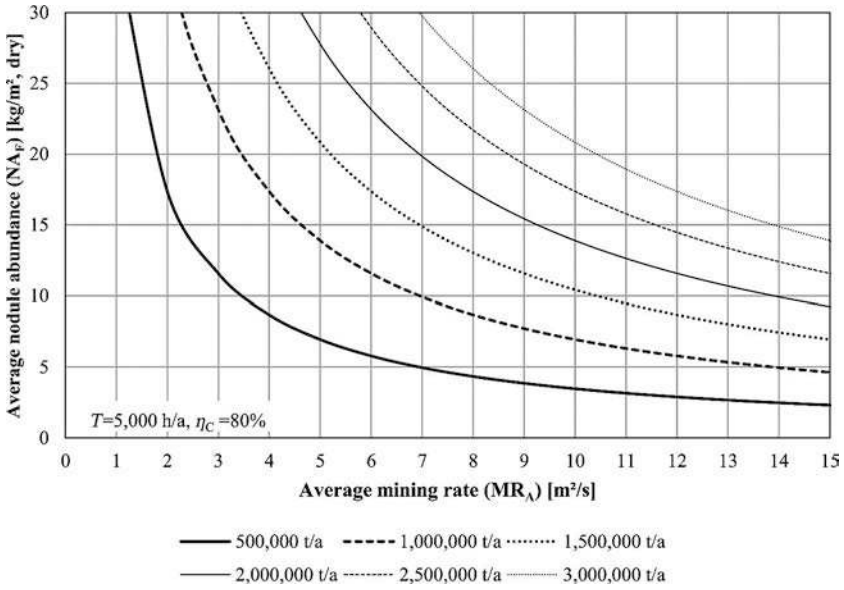

Figure 10. Annual production rate (P_A) as a function of the average mining rate (MR_A) and average abundance (NA_F) at a constant collecting efficiency (η_C) of 80% and 5,000 operating hours (T) exemplary for the Blue Mining project.

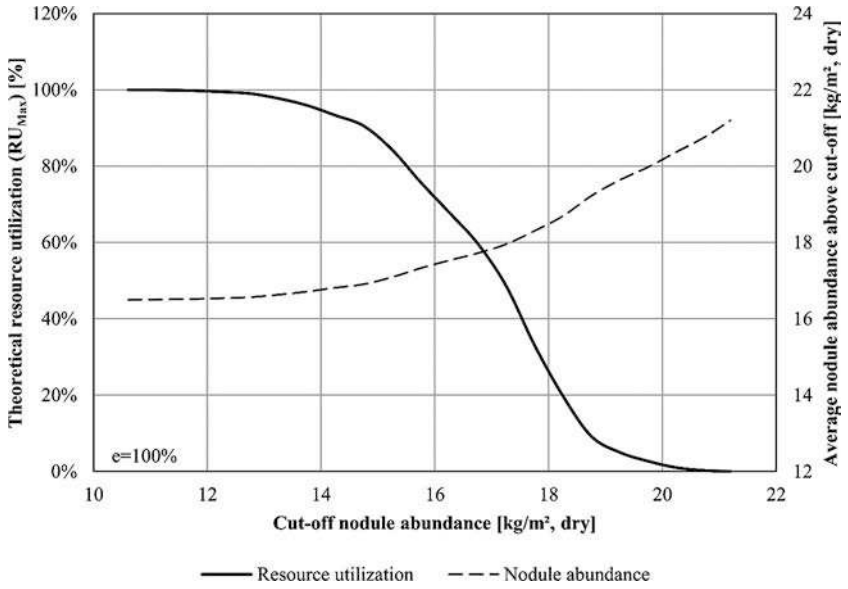

Figure 11. Theoretical resource utilization (RU_{Max}) as a function of the cutoff nodule abundance and the average nodule abundance above cutoff exemplary for the mine site of the Blue Mining project (Rahn 2016).

Table 3. Likelihood of occurrence of areas of adequate nodule abundances estimated for different annual production rates and mining rates.

	Mining rate (MR_A)[a], m²/s		
Annual production rate, P_A (Mt/a)	10	8	6
0.5	A* (3; 100%)	A* (4; 100%)	A* (6; 100%)
1.0	A* (7; 100%)	A (9; 100%)	A (12; 100%)
1.5	A (10; 100%)	A (13; 100%)	B (17; 90%)
2.0	A (14; 100%)	B (17; 90%)	C (23; 0%)
2.5	B (17; 90%)	C (22; 0%)	C (29; 0%)
3.0	C (19; 10%)	C (26; 0%)	C (35; 0%)

Classification: A* (most likely); A (likely); B (less likely); C (unlikely).
In brackets, the required nodule abundance in the mining fields NA_F (kg/m²; dry weight) and the corresponding theoretical resource utilization RU_{Max} for the exemplary mine site studied by Rahn (2016).
[a]Average mining rate (MR_A) based on 5,000 operating hours per year and a collecting efficiency of 80%.

Table 4. Mining efficiencies estimated for the study area.

Item		Values		Unit
	Derivation	Base case	Lower coverage	
A Gross mineable proportion (α)	Computed	70	70	%
B Net mineable proportion (β)	Computed	36	36	%
C Utilization of mineable area (φ)	(B/A)	51	51	%
D Area coverage performance (η_A)	Assumed	95	75	%
E Collecting efficiency (η_C)	Assumed	80	80	%
F In-field mining efficiency (η_{MF})	D × E	76	60	%
G Overall mining efficiency (η_M)	C × F	39	31	%

Discussion

The image filters to identify potentially mineable areas and results of the spatial (image) analysis are discussed. The Blue Mining concept and assumptions made to estimate key performance figures (PKFs) are only hypothetical to demonstrate the applicability of the methodology. Therefore, the discussion focuses on the assumptions and the definitions, prior than on the results.

Table 5. Seafloor consumption and requirement estimated for different annual production rates and average nodule abundances.

Item	Values				Unit
Annual production rate (P_A)	1.5	1.5	2.0	2 .0	Mt/a, dry
Average nodule abundance (NA_F)	13.7	16.5	13.7	16.5	kg/m², dry
Area consumption (A^*_M)	137	114	182	152	km²/a
Over 20 years (D)	2,700	2,300	3,600	3,000	km²
Soccer fields per day	76	64	102	85	Fields
Total seafloor requirement (A^*_{TOT}) for a duration (D) of 20 years, where $\eta_M = 30\%$ and $\alpha = 70\%$	10,400	8,700	13,900	11,500	km²
Total seafloor requirement (A^*_{TOT}) for a duration (D) of 20 years, where $\eta_M = 40\%$ and $\alpha = 70\%$	7,800	6,500	10,400	8,700	km²

Spatial analysis

A strip mining concept requires the identification of continuously mineable areas. Most software applications already provide comparable filters for this purpose, e.g., ArcGIS™. Developed filters already assume a strip-like mining pattern. This is inspired by traffic patterns of farming machines (Grisso et al. 2002; Poncet et al. 2016). The intention here is not to result in an optimal field design and mining route, but to identify continuous areas which would favor mining long, narrow strips. A circular (CIR-) filter (Figure 7a) has not proven to be efficient as narrow areas are not detected, which are potentially mineable. The bidirectional (VER-) filter (Figure 7b) is neither suitable as it would be too restrictive for future mine planning. The combined (MIX-) filter (Figure 7d) seems to be most suitable as advantages of both filters are combined. Although filter settings must be further fine-tuned, it can be pointed out that the geology favors a strip-like mining pattern. Sound criteria to differentiate nonmineable from mineable areas have still to be investigated.

Comparable to agriculture, there might be "profitable" and "less profitable" fields based on operating profit generated during the time spent in a field. The authors expect that shape, number, size, and spatial distribution of obstacles among other factors have effect on time efficiency as known from agriculture (Grisso, Jasa, and Rolofson 2000; Hunt and Wilson 2015). A mining field is expected to be shaped through the field planning process involving route planning. Field planning is only hinted in this paper. The presented mapping technique is adjusted to the expectation of the authors that pilot mining would take place in areas with a high mineable proportion (≥90%), while more disturbed areas (≥80%) may be used for turning or serve as a safety distance to threats, e.g., cliffs or protected areas of environmental interest. Further research is required concerning field planning to determine the exact shape of a mining field, mining pattern, and time to mine it. Much of this is already described for farming machines (Hunt and Wilson 2015).

Preliminary results of this paper give already an impression on how the seafloor may look like after mining took place (Figure 8). Mining would leave patchy areas scattered on the ocean seafloor (Kuhn, Rühlemann, and Wiedicke-Hombach 2012). Potential mining fields are embedded in horst and graben structures and are predefined by geology (Rühlemann et al. 2009). Considering that horizontal structures visible in the processed (filter-) images are artifacts as assumed by Rahn (2016), there may be fewer but longer fields. This cannot be clarified with the underlying data. Moreover, only about 3% of E1 was analyzed, which may not be representative for other regions inside or outside the license area. The factsheet on polymetallic nodules published by the ISA, referring to results of J. P. Lenoble for the French pioneer area, states: "In the best areas, they would be 1 to 5 km wide and 10 to 18 km long, with a north-south orientation. They might cover 35% of the bottom with a nodule abundance of 15 kg/m^2." (International Seabed Authority 2003) These dimensions are comparable to those determined in the scope of this study.

Furthermore, black pixels of the binary images may be traversable, other than assumed in this study. In addition, due to the relatively low resolution of the seafloor data, raster units can consist of nonmineable parts and vice versa. Mine planning will require a more precise prediction of seafloor properties, e.g., on nodule abundance and grades. A new approach to increase prediction confidence has been investigated by the BGR in collaboration with Beak Consultants GmbH using an algorithm of artificial neural network to compile predictive maps for SMnN coverage. Based on the prediction results, mineral resources of manganese, copper, nickel, cobalt, molybdenum, vanadium, titan, zinc, and rare earth elements were estimated at different cutoff grades (Beak consultants 2015). In addition to exploration, it is considered that AUVs/ROVs scout the seafloor during mining to update the mine plan with a spatial resolution of a few meters (Kuhn et al. 2011).

Production key figures

Results shown in this paper may not be representative for other areas or projects due to legal, economic, and technical uncertainties (ECORYS 2014). Furthermore, the analyzed area (about 1,800 km^2) accounts for only about 3% of the entire eastern German license area E1. Characteristics of the exemplary mine site differ significantly (Table 1).

Production

To achieve a certain production target, mining must focus on the areas of adequate abundance (Figure 10). Beside geological and technical reasons, production and thus the required abundance are influenced by the mining rate. The annual average mining rate depends on the mining capacity provided by the SMT(s) as well as on the time operation is performed at full mining capacity (Formula 10). Technical figures are closely related to those used in agricultural engineering (Grisso, Jasa, and Rolofson 2000; Hunt and Wilson 2015; Hanna 2016). With the provided formula (Formula 8), one could determine the necessary average abundance to realize a certain annual production rate. Then it might be possible to map out the appropriate areas on the seafloor meeting the requirements. On the other hand, based on a given annual production rate and a given abundance, one could determine the necessary mining rate (i.e., the needed technical layout and capacity of a SMT).

With respect to dimensioning, the lifting capacity of the VTS must fit to the mining capacity and peaks in nodule abundance (Figure 9). Dilution of ore with sediments and transport losses are not considered. According to the current state of the art, SMnN are freed from sediments inside the SMT (ECORYS 2014). To dimension the SMT(s), the annual operating time and time efficiency, i.e., time mining at full rated speed and full width utilization must be investigated (Formula 11). While the annual operating time (5,000 operating hours) is an experience-based figure from dredging, time efficiency is a largely unknown factor as of lacking experience. In agriculture, field efficiencies of farming machines typically range between 50 and 80% (Grisso, Jasa, and Rolofson 2000). Achieving similar performance as in farming will be an ambitious challenge.

As shown, average mining rates of 6–10 m^2/s would be required to recover 1.5–2 Mt SMnN per year. The Blue Mining reference of 2 Mt SMnN per year is based on an early economic assessment. Although a collecting efficiency of 80% was assumed, it is not a constant. It depends, inter alia, on the colleting speed, nodule abundance, and collecting technology (Handschuh et al. 2001).

Adopting the mentioned time efficiencies to SMnN mining, a total capacity of about 7.5–20 m^2/s would be required. In contrast to this wide range, a mining capacity of 9 m^2/s is considered by Blue Mining (Table 2). The MH Wirth concept is similar to the proposed Blue Mining concept and consists of two SMTs (Kuhn et al. 2011). Their SMTs are equipped with two drums, each 6 m in width. The nominal (conceptual) operating speed is 0.5 m/s. In comparison, the Claas Lexion 780, one of the world's biggest combine harvesters, is equipped with six drums, each 1.7 m in width (Claas 2017). The nominal operating speed according to data specifications is 3 m/s.

Small-scale and prototype tests were performed in the past in shallow waters (Deepak et al. 2001; Hong et al. 2010). Further research and tests are necessary to resolve uncertainties. It has yet to be investigated if mining rates can be achieved, which would ensure performing SMnN mining in

a balanced manner: Ensuring profitability at acceptable resource utilization and reasonable seafloor consumption. In the opinion of the authors, an annual production rate of 2 Mt or higher seems to be too optimistic to expect from a pioneer-mining operation, mainly due to geological, technical, and operational reasons.

Resource utilization

Resource utilization is depending on the annual production rate and the average mining rate (Table 3). Within the scope of this paper, the theoretical resource utilization (RU_{Max}) was estimated for an exemplary area, indicating the mining potential. In practice, the resource utilization is probably lower due to mining losses (considered in the extraction efficiency). According to Kuhn, Rühlemann, and Wiedicke-Hombach (2012), E1 has proven to consist of at least 10 kg/m^2 (wet weight). This corresponds to a dry weight of about 7 kg/m^2. The letter A (likely) indicates that the required average abundance is less than or equal to 14 kg/m^2 (dry weight). This value refers to an average abundance of 13.7 kg/m^2 assessed for E1 (Rühlemann et al. 2011). Feasibility studies performed in the 1970s and 80 s used similar nodule abundances for their calculations (Nyhart et al. 1978; Hillman and Gosling 1985). The letter B (less likely) is referring to average abundances between 14 and 17 kg/m^2. Large continuous areas with abundances in this range are expected to be representative for future mining fields (Figure 2). All values above 17 kg/m^2 are marked with a C (unlikely), expecting that only a small proportion of the seafloor contains abundances in this range. Only mining nodule-rich parts of a mineral deposit, labeled with C, is expected to result in poor resource utilization.

Resource utilization as the share of the deposit actually used can be applied as an indicator to assess the sustainability of a mining operation. Without legal regulations, high production requirements and mining rates below expectations could foster cherry picking, mining only the favorable parts of a deposit, not utilizing the mineral resource well. Since metal grades have shown to be relatively constant, these parts would be nodule-rich areas and those easy to mine, i.e., resulting in higher average mining rates. Since the spatial distribution of SMnN is site specific, the classification matrix (Table 3) may not apply for other areas. However, it may be useful to get the first, general idea on what can be expected with regard to the spatial distribution in the CCZ (International Seabed Authority 2010).

Mining and extraction efficiency

After UNOET (1987), "mining efficiency" or "overall efficiency" is the product of the collecting efficiency (originally referred to "dredge efficiency") and area coverage performance (originally referred to "sweep efficiency"). At that time, a dredge head was expected to be dragged over the seafloor to collect SMnN. The overall efficiency was estimated to range most likely between values of 10 and 40% (UNOET 1987). In comparison to their concept, the Blue Mining approach is inspired by the potato harvest on land. One or several self-propelled, crawler-type SMTs are planned to be navigated along predefined routes as state of the art (ECORYS 2014). However, in both cases, the mineable area must be defined in a first instance. Other than assumed for the former mine site concept, the mineable proportion is expected to be narrowed down due to field design. Therefore, it is suggested to consider the degree of utilization and to differentiate between in-field and overall mining efficiency to consider field design.

Field design is a subsequent planning process, closely related to route planning. An area (referring to a specific raster unit) can meet the criteria of being mineable but may not be mined. Path planning is subject of many scientific papers and is related to coverage problems (Huang 2001; Galceran and Carreras 2012). However, the main objective is not only to best cover the mineable area but to result in a (most) economic route, i.e., mining pattern, while considering the affected area (to be explained). Although, if a "good utilization" is aimed, it is yet not certain if a strip-like mining pattern is realizable. It might be the case, that the SMT cannot be navigated as precisely as known from precision-farming operations in agriculture, resulting in a poor area coverage performance. In conclusion, a pilot-mining test has yet to demonstrate the technical feasibility of strip mining and SMnN mining in general.

The extraction efficiency or extraction ratio is an established term in mining, which is commonly used in room-and-pillar mining (Darling 2011). Room-and-pillar mining is an underground mining method, which is usually used for flat-lying deposits. The material is extracted across a horizontal plane, whereby pillars are left in place to support the roof. SMnN can be considered as a thin layer of ore covering vast areas of seafloor. Although, the reasons for not mining valuable material are different, deep-sea strip mining and terrestrial room-and-pillar mining have in common that mine design has effect on extraction efficiency. In SMnN mining, the extraction efficiency is defined to be the ratio of the quantity of SMnN mined to the reserve. Cherry picking only nodule-rich parts of a mine site could result in poor mining efficiency but sufficient (higher) extraction efficiency at the same time. For the exemplary area, extraction efficiency was estimated to be 30–50%, while the overall mining efficiency was computed to be 40% at the best. However, the difference is insignificant in case the mineable area is utilized most efficiently.

Reserve estimation

In this paper, SMnN contained in the mineable area are qualified as potential reserves. The purpose was to investigate the requirements and dimensions of a future SMnN system, which would utilize the deposit in the best possible manner. None of the known SMnN resources have reached the status of a reserve, yet. This is mainly due to the absence of a regulatory framework and poor technical readiness level (ECORYS 2014). A standard to report SMnN reserves has not been established, yet. For the mining entrepreneur, it will be important to validate if a field generates enough profit in adequate time taking into account technical feasibility and field characteristics. Still, that does not exclude a field from turning into a reserve at some later point in time. Therefore, it is suggested to report the quantity of SMnN in the mineable area and additionally the quantity of SMnN in the mining fields, after field design and economic assessment.

Duration of mining

The analyzed part of E1 (about 1,800 km^2) may already provide enough SMnN to sustain mining for maybe 2½–5½ years. Planning with at least 20 years of production, another 3–7 areas would be required of similar characteristics. Under the premise that the area is representative for the entire license area E1 (Table 1), one mining operation (one MSV) could be performed for maybe 84–186 years under the assumption that 30–50% of the resource is recovered. However, these figures are very speculative. Kuhn, Rühlemann, and Wiedicke-Hombach (2012) identified 10 prospective fields in E1, which "[…] cover 18% of the total area and contain nodule reserves that sustain at least 40 years of seabed mining." The term field refers here to the potentially mineable area, not considering extraction efficiency. In conclusion, results indicate that extraction efficiency and thus field design will have effect on the life of mine and number of mining projects per license area and thus needs to be thoroughly studied.

Seafloor consumption and requirement

The terms land (seafloor) consumption and requirement are common terms in agriculture (Hunt and Wilson 2015) The formula provided to estimate the seafloor requirement (Formula 20) is similar to the one proposed by the UNOET (1987). They estimated that mining would require approximately 15,300–125,000 km^2 over a period of 20–40 years at a production of 3 Mt per year. "The wide range in the estimates is primarily due to the different perceptions of the risk factors involved." (UNOET 1987) In comparison, E1 is about 58,000 km^2 in size. Our estimations indicate that about 6,500–13,900 km^2 of seafloor would be needed to sustain a single mining operation of 20 years at 1.5–2 Mt SMnN per year. Even if the annual production rate and overall mining efficiency are marked by uncertainty, a requirement of 125,000 km^2 of seafloor cannot be expected for E1: 80% of the exploration area is of flat terrain ($\leq$3°) and the average nodule abundance is 13.7 kg/m^2 (dry weight) (Rühlemann et al. 2009).

Environmental aspects

Seafloor manganese nodule mining is predicted to disturb vast areas of seafloor (Thiel and Schriever 1993). Simulations have shown that sediment particles can settle over distances of several to hundreds of kilometers and may form a thin sediment layer which can overlap and suppress the benthic ecosystem (MIDAS 2016). Sediment is expected to be swirled up by the SMT(s). Another source is the return line ("downer"). Seawater and residue from the dewatering process on board of the MSV, basically undersized particles, are rejected into the sea (Oebius et al. 2001). Beside plume generation, the seafloor is likely to be disturbed due to the removal of SMnN and compaction of soil, which functions as habitat for sessile organisms (Valsangkar 2003; Sharma 2013). The "affected area" is a possible indicator to take the environmental footprint into consideration. It is defined as by the deep-sea mining-disturbed seafloor implying the, yet to define, severity of impact (Volkmann 2014). To present, there are no environmental provisions due to the absence of a regulatory framework. Also, there is still a lack in understanding the large-scale and long-time environmental impact of deep-sea mining. In conclusion, the affected area cannot be quantified, yet.

Other mining concepts

Beside the Blue Mining concept, there are others—due to the absence of regulations—yet not competing mining concepts, such as the Indian for instance. The University of Siegen, Germany proposed in collaboration with the National Institute of Ocean Technology, India a concept for deep-sea mining based on a flexible riser and self-propelled mining machines (Handschuh et al. 2001). In contrast to the Blue Mining concept, the Indian system operates (semi-) stationary. Instead of a continuously moving MSV, platforms are considered, from which numerous smaller SMT(s) are operated at speeds of 0.2 m/s and collecting efficiencies of 70%. The platform would have to be moved by 2 km approximately every six weeks. In the beginning four to five platforms would be required to lift one million wet metric tons of nodules. It is considered that production could be increased to one million tons per platform. Today, no statement can be made which of the mentioned concepts is the better one, considering environmental, technical, and economic aspects. An environmental impact assessment through a pilot-mining test could provide that (International Seabed Authority 2013).

Conclusion

Potential mining fields can be found in plain areas embedded in horst and graben structures. Bulk-mining would leave patchy areas scattered on the seafloor. In the case of eastern German license area, the geology favors a strip-like mining pattern in NNE-SSW direction. Production from a single Blue Mining or comparable system is likely limited to 1.5–2 Mt SMnN per year, mainly due to geological, technical, and operational reasons. Time efficiency, i.e., annual operating time at full mining capacity has emerged to be the largest unknown factor to access future mining systems. Further research and pilot-mining tests are necessary to gain a better understanding of the geology, technical, and economic feasibility and environmental footprint of SMnN mining. Although results are marked by uncertainty, the presented mapping technique and provided formulas to calculate PKFs are a step forward to technically and economically dimension an SMnN mining system. Parallels to agricultural engineering regarding machine, land, and resource management become obvious.

Acknowledgments

The authors thank Mirjam Rahn (RWTH Aachen University) who prepared the deposit model in the framework of the Blue Mining project. Exploration data were kindly provided by the German "Federal Institute for Geosciences and Natural Resources" (BGR) where we would like to thank Dr Thomas Kuhn for good discussions and exchange of knowhow. Furthermore, we would like to thank Prof. Ludger Rattmann (THGA Bochum, Germany) for initial discussions and proposals on the topic of deep-sea mining and Prof. Bernd Lottermoser (RWTH Aachen University) for additional inputs and a critical review of our manuscript.

Funding

This work received funding by the European Commission as part of the 7th Framework Programme for Research and Technological Development (GA No. 604500).

References

Beak consultants. 2015. Advangeo® predicts sea floor manganese nodule resources: Successful cooperation between Beak and the Federal institute for geosciences and natural resources of Germany. http://www.beak.de/beak/en/new_02_dec_2015 (accessed June 21, 2016).

Claas. 2017. LEXION 780–740: Technische Daten. http://www.claas.de/produkte/maehdrescher/lexion780-740-2016/technische-daten (accessed March 22, 2017).

Darling, P. 2011. *SME mining engineering handbook, 3rd ed*. Englewood: Society for Mining, Metallurgy, and Exploration.

Deepak, C. R., M. A. Shajahan, M. A. Atmanand, K. Annamalai, R. Jeyamani, M. Ravindran, E. Schulte, R. Handschuh, J. Panthel, and H. Grebe eds. 2001. *Developmental tests on the underwater mining system using flexible riser concept*. International Society of Offshore and Polar Engineers, Szczecin, Poland.

ECORYS. 2014. Study to investigate state of knowledge of deep-sea mining: Final Report under FWC MARE/2012/06 - SC E1/2013/04. https://webgate.ec.europa.eu/maritimeforum/en/node/3732 (accessed November 26, 2016).

Galceran, E., and M. Carreras. 2012. Efficient seabed coverage path planning for ASVs and AUVs. 2012 IEEE/RSJ international conference on intelligent robots and systems (IROS 2012), Vilamoura-Algarve, Portugal, October 7–12, 2012, 88–93. Piscataway, NJ: IEEE.

Glasby, G. P. 2002. Deep seabed mining: Past failures and future prospects. *Marine Georesources & Geotechnology* 20 (2):161–76. doi:10.1080/03608860290051859

Grisso, R. D., P. J. Jasa, and D. E. Rolofson. 2000. Field efficiency determination from spatial data. Written for presentation at the 2000 ASAE annual international meeting sponsored by ASAE. Paper Number 001013. Department of Biological Systems Engineering, University of Nebraska, Milwaukee, Wisconsin, USA.

Grisso, R. D., P. J. Jasa, and D. E. Rolofson. 2002. Analysis of traffic patterns and yield monitor data for field efficiency determination. *Applied Engineering in Agriculture* 18 (2):171–78. doi:10.13031/2013.7782

Handschuh, R., H. Grebe, J. Panthel, E. Schule, B. Wenzlawiak, W. Schwarz, M. A. Atmanand, R. Jeyamani, M. A. Shajahan, C. R. Deepak, and M. Ravindran. 2001. Innovative deep ocean mining concept based on flexible riser and self-propelled mining machines. The proceedings of the fourth (2001) ISOPE ocean mining symposium, ed. by The International Society of Offshore and Polar Engineers (ISOPE), 99–107. Cupertino, CA: International Society of Offshore and Polar Engineers.

Hanna, M. 2016. Estimating the field capacity of farm machines. http://lib.dr.iastate.edu/cgi/viewcontent.cgi?article=1003&context=pubs_agdm (accessed January 9, 2017).

Hein, J. R. 2013. Manganese nodules. In *Encyclopedia of marine geosciences*, ed. by J. Harff M. Meschede S. Petersen and J. Thiede 1–7. Dordrecht: Springer Netherlands.

Hein, J. R. 2016. Manganese nodules. In *Encyclopedia of marine geosciences*, ed. by J. Harff M. Meschede S. Petersen and J. Thiede 408–12. Encyclopedia of earth sciences series. Dordrecht: Springer Reference.

Hillman, T., and B. B. Gosling. 1985. *Mining deep ocean manganese nodules: Description and economic analysis of a potential venture*. Washington, D.C.: U.S. Department of the Interior.

Hong, S., J.-S. Choi, J.-H. Kim, and C.-K. Yang eds. 1999. *Experimental study on hydraulic performance of hybrid pick-up device of manganese nodule collector*. Goa, India: International Society of Offshore and Polar Engineers.

Hong, S., H.-W. Kimg, J.-S. Choi, T.-K. Yeu, S.-J. Park, C.-H. Lee, and S.-M. Yoon. 2010. A self-propelled deep-seabed miner and lessons from shallow water tests. Proceedings of the ASME 29th international conference on ocean, offshore and arctic engineering 2010, 75–86. New York: ASME.

Huang, W. H. 2001. Optimal line-sweep-based decompositions for coverage algorithms. Proceedings: 2001 ICRA, IEEE international conference on robotics and automation, May 21–26, 2001, COEX, Seoul, Korea, 27–32. Piscataway, NJ: IEEE Operations Center.

Hunt, D., and D. Wilson. 2015. *Farm power and machinery management*. Long Grove, Illinois: Waveland Press.

International Seabed Authority (2003). Polymetallic nodules. Brochure. www.isa.org.jm/documents-resources/publications (accessed October 24, 2016).

International Seabed Authority ed. 2010. A geological model of polymetallic nodule deposits in the clarion Clipperton fracture zone. Technical Study 6.

International Seabed Authority ed. 2013. Towards the development of a regulatory framework for polymetallic nodule exploitation in the area. Technical Study 11.

Knodt, S., T. Kleinen, C. Dornieden, J. Lorscheidt, B. Bjørneklett, and A. Mitzlaff. 2016. Development and engineering of offshore mining systems - State of the art and future perspectives. Houston, Texas, USA: Offshore technology conference.

Kuhn, T., C. Rühlemann, and M. Wiedicke-Hombach. 2012. Developing a strategy for the exploration of vast seafloor areas for prospective manganese nodule fields. In *Marine minerals: Finding the right balance of sustainable development and environmental protection*, ed. by H. Zhou and C. L. Morgan 9. Shanghai.

Kuhn, T., C. Rühlemann, M. Wiedicke-Hombach, J. Rutkowsky, H. J. Wirth, D. Koenig, T. Kleinen, and T. Mathy. 2011. Tiefseeförderung von Manganknollen. *Schiff & Hafen* 5:78–83.

Marscheider-Weidemann, F., S. Langkau, T. Hummen, L. Erdmann, L. A. Tercero Espinoza, G. Angerer, M. Marwede, and S. Benecke. 2016. *Rohstoffe für Zukunftstechnologien 2016: Auftragsstudie*. DERA Rohstoffinformationen 28. Hannover: DERA.

Mero, J. L. 1977. Chapter 11 economic aspects of nodule mining. In *Marine manganese deposits*, ed. by G. P. Glasby vol. 15, 327–55. Elsevier Oceanography Series 15. Amsterdam: Elsevier.

MIDAS. 2016. Managing impacts of deep sea resource exploitation: Research highlights. http://www.eu-midas.net/library (accessed November 25, 2016).

Nyhart, J. D., L. Antrim, A. E. Capstaff, A. D. Kohlert, and D. Leshawm. 1978. A cost model of deep ocean mining and associated regulatory issues. Sea Grant Program.

Oebius, H. U., H. J. Becker, S. Rolinski, and J. A. Jankowski. 2001. Parameterization and evaluation of marine environmental impacts produced by deep-sea manganese nodule mining. *Deep-Sea Research II* 48:1453–3467. doi:10.1016/s0967-0645(01)00052-2

Poncet, A., J. Fulton, K. Port, T. Mcdonald, and G. Pate. 2016. Optimizing field traffic patterns to improve machinery efficiency: Path planning using guidance lines. http://ohioline.osu.edu/factsheet/fabe-5531 (accessed January 09, 2017).

Rahn, M. 2016. Deliverable 3.11: Deposit models. Public report submitted to the EU Commission within the 7th framework programme (GA No. 604500). http://www.bluemining.eu/downloads/ (accessed July 26, 2016)

Rendu, J.-M., and N. Miskelly. 2013. Mineral resources and mineral reserves: Progress on international definitions and reporting standards. *Mining Technology* 110 (3):133–38. doi:10.1179/mnt.2001.110.3.133

Rühlemann, C., U. Barckhausen, S. Ladage, L. Reinhardt, and M. Wiedicke eds. 2009. *Exploration for polymetallic nodules in the German license area*. Chennai, India: International Society of Offshore and Polar Engineers.

Rühlemann, C., T. Kuhn, A. Vink, and M. Wiedicke. 2013. *Methods of manganese nodule exploration in the German license area*. Rio de Janeiro: UMI.

Rühlemann, C., T. Kuhn, M. Wiedicke-Hombach, S. Kasten, K. Mewes, and A. Picard. 2011. Current status of manganese nodule exploration in the German license area. *The proceedings of the ninth (2011) ISOPE*

ocean mining symposium, ed. Maui, Hawaii, USA: The International Society of Offshore and Polar Engineers (ISOPE), 168–73.

SAP. 2014. SAP Integrated business planning: Production. http://help-legacy.sap.com/downloads/pdf/saphelp_ibp1608_en_be_9136565b0ec44ee10000000a44147b_content.pdf (accessed March 21, 2017).

Sharma, R. 2013. Deep-sea impact experiments and their future requirements. *Marine Georesources & Geotechnology* 23 (4):331–38. doi:10.1080/10641190500446698

Stuart, E. 2011. What is multibeam backscatter?. http://oceanexplorer.noaa.gov/okeanos/explorations/ex1104/logs/aug12/aug12.html (accessed March 06, 2017).

Thiel, H., and G. Schriever. 1993. Environmental consequences of deep-sea mining. *International Challenges* 13:54–70.

United Nations. 1982. United Nations convention on the law of the sea: UNCLOS. http://www.un.org/depts/los/convention_agreements/texts/unclos/unclos_e.pdf (accessed November 18, 2016).

UNOET, ed. 1987. *Delineation of mine sites and potential in different sea areas*, vol. 9. Seabed Minerals Series 4. London: Graham & Trotman.

Valsangkar, A. B. 2003. Deep-sea polymetallic nodule mining: Challenges ahead for technologists and environmentalists. *Marine Georesources and Geotechnology* 21 (2):81–91. doi:10.1080/716100481

Volkmann, S. 2014. Deliverable 3.21: Sustainable indicators. Public report submitted to the EU Commission within the 7th Framework Programme (GA No. 604500). http://www.bluemining.eu/downloads/ (accessed July 26, 2016).

Wiedicke, M., T. Kuhn, C. Rühlemann, and A. Vink. 2015. Schwarz-Schampera: Deep-sea mining–A future source of raw materials. Mining Report 151.

Yamazaki, T. ed. 2008. Model mining units of the 20th century and the economies. *Technical paper for ISA Workshop on Polymetallic Nodule Mining Technology - Current Status and Challenges Ahead*; Feb. 18-22, 2008, Chennai, India.